Spectroscopic and cytotoxic studies of losartan complexes

Mansoor Ahmed[1], Mohsin Ali[2*], Syed Imran Ali[3], Majid Mumtaz[2], Syed Moazzam Haider[4], Shakil Ahmed[4], Khalid Mohammed Khan[4,7], Muhammad Asad Khan Tanoli[2], Seyed Abdulmajid Ayatollahi[5] and Nasir Ansar[6]

[1]Department of Pharmaceutical Chemistry, Faculty of Pharmacy and Pharmaceutical Sciences, University of Karachi, Karachi, Pakistan
[2]Department of Chemistry, University of Karachi, Karachi, Pakistan
[3]Department of Applied Chemistry & Chemical Technology, University of Karachi, Karachi, Pakistan
[4]HEJ Research Institute of Chemistry International Center for Chemical and Biological Sciences, University of Karachi, Karachi, Pakistan
[5]Phytochemistry Research Center and Department of Pharmacognosy, School of Pharmacy, Shahid Beheshti University of Medical Sciences, Tehran, Iran
[6]Director General Education Department, Govt. of Sindh, Pakistan
[7]Department of Clinical Pharmacy, Institute for Research and Medical Consultations (IRMC), Imam Abdulrahman Bin Faisal University, PO Box 31441, Dammam, Saudi Arabia

Abstract: Use of drug-metal complexes for the treatment of several human diseases has resulted in significant progress in the field of medicinal inorganic chemistry. The current study describes the synthesis and characterization of Cu (II) and Ni (II) complexes of *Losartan*, an antihypertensive drug. These complexes were evaluated for their cytotoxic activity against four human cancer cell lines; SNB-19, HCT-15, COLO-205 and KB-3-1. Spectroscopic characterization revealed that during complex formation, the metal was bound through the nitrogen atoms of the tetrazole moiety of the losartan molecule. The molecular formulas of copper ($[Cu\ (LS)_2\ Cl_2].6H_2O$) and nickel ($[Ni\ (LS)_2Cl_2].\ H_2O$) complexes were found to be in agreement with the analytical data obtained through elemental analysis. For both the complexes, metal to ligand ratios of 1:2 were calculated. As revealed by FTIR, UV-Visible, and ^{1}H-NMR studies, both the complexes displayed octahedral geometries. Scanning electron microscopy (SEM) revealed marked changes in the morphology of the complexes, compared to the pure drug. From XRD studies, characteristic crystalline peaks of pure losartan were observed whereas no prominent peaks were observed for its complexes. Complexes were found to be inactive in the cytotoxic activity test performed using SNB-19, HCT-15, COLO-205 and KB-3-1 cell lines.

Keywords: SEM, SNB-19 cell line, HCT-15 cell line, COLO-205 cell line, KB-3-1 cell line and Losartan.

INTRODUCTION

Hypertension is among the major contributors that cause progression of chronic renal diseases (Brazy *et al*., 1989, Campese VM 1991, Hannedouche *et al*., 1993, Walker 1993). An important contributor for the pathogenesis of hypertension is the renin-angiotensin system (RAS) (Griendling *et al*., 1993). Angiotensin II acts on multiple organs of the body generating reactive oxygen species (Mehta *et al*., 2007) promoting vasoconstriction, the adrenal release of aldosterone, and the activation of sympathetic nerve discharge, ultimately increasing the blood pressure (Qin 2008).

Angiotensin receptor blockers such as losartan selectively inhibits the rennin angiotensin system by specifically targeting the angiotensin II AT1 receptor and is widely used for the treatment of hypertension in humans (Wong *et al*., 1991, Timmermans PB 2009). As its mode of action is the vasodilatation of blood vessels, it therefore reduces the blood pressure. It is an orally active, highly specific and competitive antagonist of angiotensin II to the AT1 receptor subtype (Johnston 1995). It undergoes carboxylation metabolism which results in the formation of an active metabolite, E-3174 and several inactive metabolites. Both, parent compound and its active metabolite are highly protein bound and irremovable by hemodialysis (Wong *et al*., 1990, Ska *et al*., 1995). Recent studies demonstrated that losartan considerably obstruct tumor growth and considered to be very effective in the treatment of tumors (Rhodes *et al*., 2009, Chauhan *et al*., 2013). It reduces compression within the tumors by releasing physical forces exerting on blood vessels. The resulting open blood vessels can be used effectively to kill the tumor cells by delivering sufficient concentrations of chemotherapeutic agents to this target tissue.

Despite all these benefits of losartan, there are still some limitations that need to be overcome. For instance, many researchers reported various side effects such as nausea, fatigue, weakness, and breathing problems (Lacourcière *et al*., 1994, Dickstein *et al*., 1995, Tedesco *et al*., 1998). Endeavors to explore new strategies and formulations to improve efficiency and efficacy of losartan are justified owing its increasing clinical and commercial importance.

**Corresponding author:* e-mail: mohsin.ali@uok.edu.pk

The pharmaceutical applications of metal complexes showed excellent potential and thus gaining increasing clinical and commercial importance. These compounds offer new possibilities to design therapeutic formulations to mitigate the inherent limitations of the conventional formulations. Although some progress have been made for the synthesis and medicinal applications of losartan-metal complexes (Etcheverry *et al*., 2007); further research to explore their physicochemical properties, molecular characterization and biochemical activity is required. For instance, copper is one of the relatively small group of metals which are essential to health and exhibits considerable biochemical action (Iakovidis *et al*., 2011). As an endogenous metal, it is considered to be less toxic and therefore Cu (II)-based complexes simulated an ever-increasing research interest as promising candidates for therapeutic applications in anticancer therapy (Ferrari *et al*., 2001, Belicchi *et al*., 2002, Rodrìguez-Argüelles *et al*., 2004). The biological significance of nickel is also well-known owing to its presence in many enzymes (Andrews RK 1988, Meyer F 2003). The biological activity of Ni(II) complexes with various ligands such as vitamins, antitumor, antibiotics, anticonvulsant, antioxidant, antileishmanial, antiproliferative and antiepileptic agents have been also reported (Kurtaran *et al*., 2005, Yeşilel *et al*., 2006, Skyrianou *et al*., 2009, Skyrianou *et al*., 2011, Sathyadevi *et al*., 2012, Alomar *et al*., 2013, Hsu *et al*., 2013, Shawish *et al*., 2014).

In the current research work, we report synthesis, spectral and morphological characterization of copper and nickel complexes of losartan and evaluate their potential cytotoxic activity using SNB-19, HCT-15, COLO-205 and KB-3-1 cell lines. For the complex formation with losartan, two metals copper and nickel were selected due to their significance in biological systems and considerable biochemical action either as essential metals or as a constituent of various drug formulations (Osredkar *et al*., 2011). The spectroscopic characterization revealed successful formation of the complexes with an octahedral geometry where the metal is bound through the nitrogen atoms of the tetrazole moiety of the losartan molecule. The complexes were further investigated to explore their morphology and cytotoxic activity.

MATERIALS AND METHODS

Losartan potassium (LS) was gratis from Brooks Pharma (Pvt) Ltd, Karachi, Pakistan. The copper and nickel used in the form of hydrated chlorides. Methanol and dimethylsulfoxide (DMSO) were of analytical grade and procured from Merck, Germany.

Synthesis of the complexes

First, 0.1 M stock solutions of losartan (LS), $CuCl_2$ and $NiCl_2$ were prepared in methanol. A 20.0 mL portion of LS solution was then transferred in a round bottom flask followed by slow addition of $CuCl_2$ solution with continuous stirring. The mixture was then refluxed for 3-4 hours with continuous stirring. Upon cooling, a solid metal complex was formed which was filtered, washed several times with warm methanol and dried at 60°C in an oven. The same procedure was adopted for the synthesis of nickel complex but solid complex was obtained after three days of slow evaporation at room temperature. The difference in the formation procedure of the two complexes arises because of their solubilities reaction medium.

Characterization

Elemental analysis (CHN) was carried out on a Perkin Elmer 2400 Series II elemental analyzer. FTIR spectra were recorded in KBr pellets on a Shimadzu Prestige-21 spectrophotometer in the range of 4000-400 cm^{-1}. UV-visible spectra were recorded on a Shimadzu UV-1601 spectrophotometer in DMSO solvent. ^{1}H-NMR spectra of ligand and its complexes were recorded in DMSO-d_6 on an Avance AV-400 MHz spectrometer using TMS as an internal standard. Metals were estimated by AA spectrophotometer PerkinElmer AAnalyst 700. SEM images were recorded by Scanning Electron Microscope, Jeol Japan model no. JSM6380A. Prior to imaging, the samples were coated using an auto-coater Jeol Japan model no. JFC1500. Magnetic susceptibility measurements were performed at room temperature using a Mark 1 magnetic susceptibility balance from Sherwood Scientific. Pascal's constants were used to apply diamagnetic corrections for complexes. Conductivity and pH of 0.5% solutions of complexes were measured in DMSO by conductivity meter, Janway 4071 and Metller Toledo MP220 pH meter, respectively. Melting points of ligand and its metal complexes were recorded using Stuart SMP3 melting point apparatus and are uncorrected. X-ray diffraction studies were performed using a Bruker AXS D8 (Germany) X-ray diffractometer equipped with a Cu-Kα1 radiation (1.54 Å). The data were recorded at a scanning speed of 5°/min in the range of $10^\circ < 2\theta < 60^\circ$ using a step size of 0.02°/point at 40 kV and 60 mA. All samples were analyzed as dry powder.

Cell lines and cell culture

Four cancer cell lines were selected to access the cytotoxicity of the compounds. The human astrocytoma SNB-19 cell line, human Dukes' type C colorectal adenocarcinoma HCT-15 cell line, human Dukes' type D colorectal adenocarcinoma COLO-205 cell line, and human cervix carcinoma KB-3-1 cell line were purchased from the American Type Culture Collection (ATCC, Manassas, VA). All the cell lines were cultured in DMEM supplemented with 10% FBS and 1% penicillin/ streptomycin in a humidified incubator at 37°C with 5% CO_2.

Cytotoxicity assay

A modified MTT assay was conducted to access the cytotoxicity of LS and two metal complexes of LS to

Table 1: Percentage comparison of theoretical and practical values

Compound	% C	% H	% N	%Metal
	Theoretical / Practical	Theoretical / Practical	Theoretical / Practical	Theoretical / Practical
[Cu (LS-K)$_2$Cl$_2$].6H$_2$O*	48.60 /47.75	5.52 /5.39	15.46 /15.75	5.85 /5.83
[Ni (LS-K)$_2$Cl$_2$].H$_2$O**	53.14 /53.79	4.63 /4.79	16.90 /16.85	5.90 /6.08

*M. mass 1086.37 g/mole, **M. mass 993.51 g / mole.

Table 2: Basic physical properties of LS and its metal complexes

Compound	Color	M.P. (°C)	BM	pH 0.5%	Cond. (mS)0.5%	Solubility
LS-K	Off White	184 D ± 2	-	-	-	H$_2$O, CH$_3$OH, DMF and DMSO
Cu(II)-LS	Dull green	205 D ± 2	1.81	7.3	0.02	DMF and DMSO
Ni(II)-LS	Purple blue	210 D ± 2	2.98	7.1	0.03	H$_2$O, DMF and DMSO

Table 3: Cytotoxicity of LS-K and its metal complexes on four human cancer cell lines

	IC$_{50}$ ± STD (μM)			
Drug #	SNB-19	HCT-15	COLO-205	KB-3-1
LS-K	>100	>100	>100	88.66±7.33
Cu(II)-LS	>100	>100	>100	>100
Ni(II)-LS	>100	>100	>100	>100

Data represents the mean IC$_{50}$ values for each cell line ± SD obtained from three independent sets of experiments.

cultured cancer cells. The assay assesses cell viability by detecting the formazan product formed from the reduction of 3-(4,5-dimethylthiazole-2-yl)-2,5-biphenyl tetrazolium bromide (MTT) by mitochondrial succinate dehydrogenase of metabolically active cells (Carmichael *et al*., 1987) all the four cell lines were seeded in 96-well plates at a final density of 5 x 10^3 cells/well and allowed to adhere and grow for 24 hours. After then, various concentrations of the six compounds were added respectively to the cells for 72-hour continuous drug incubation. At the end of the 68th hour of incubation, 20 µl MTT (4 mg/ml) was added to each well. The plates were incubated at 37°C for another 4 hours. Subsequently, the medium was aspirated carefully and 100 µl of DMSO were added to dissolve the formazan crystals. After shaking the plates for 5 minutes, the absorbance at 570 nm was measured using the accuSkan™ GO UV/Vis Microplate Spectrophotometer (Fisher Sci., Fair Lawn, NJ). The cytotoxicity of the compounds was represented by the calculated IC$_{50}$ (concentration that inhibited the survival of cells by 50%) values.

RESULTS

The metal complexes were synthesized by refluxing appropriate amounts of ligand and metal salts. The compositions of synthesized Cu and Ni complexes of LS are listed in table 1. These values were determined using CHN analyzer and atomic absorption spectroscopy and are in close agreement with the theoretical values. From this data, a metal-to-ligand ratio of 1:2 can be calculated for both the complexes.

Physical characteristics of the ligands and its complexes are listed in table 2. FTIR data is presented in fig. 1. The details of UV-Visible, ^{1}H-NMR, SEM and X-Ray diffraction data are mentioned in fig. 2, fig. 3, fig.4 and fig. 5 respectively. Whereas cytotoxicity date are cited in table 3.

DISCUSSION

Physicochemical properties

The Cu and Ni complexes of LS were colored and melted at higher temperatures compared to the pure losartan which clearly indicates that the formation of complexes was successful. The pH value of around 7 indicates that both the complexes are neutral. The solubility of the metal complexes was compared with the ligand by dissolving them in solvents of different polarities such as water, methanol, DMF and DMSO. The ligand was soluble in majority of solvents, whereas the two complexes were found to be insoluble in methanol. Besides, the Cu complex was only soluble in DMF and DMSO, and Ni complex was soluble in water DMSO, and DMF. This indicates that the complexes are likely to be less polar compared to the pure ligand. The obtained values of conductivity (measured in DMSO using of 0.5% solutions, table 2) indicates that the complexes possesses non-electrolytic nature suggesting that no salt anion is present outside the co-ordination sphere.

FTIR spectra

The FTIR spectra of LS-H, LS-K, LS-Cu and LS-Ni were recorded and compared to gain firsthand information about the complex formation process. The obtained data is presented in fig. 1. The infrared absorption bands in LS-H spectra observed at 3372, 1431-1417 and 1081 cm^{-1} correspond to the strong stretching and bending N-H

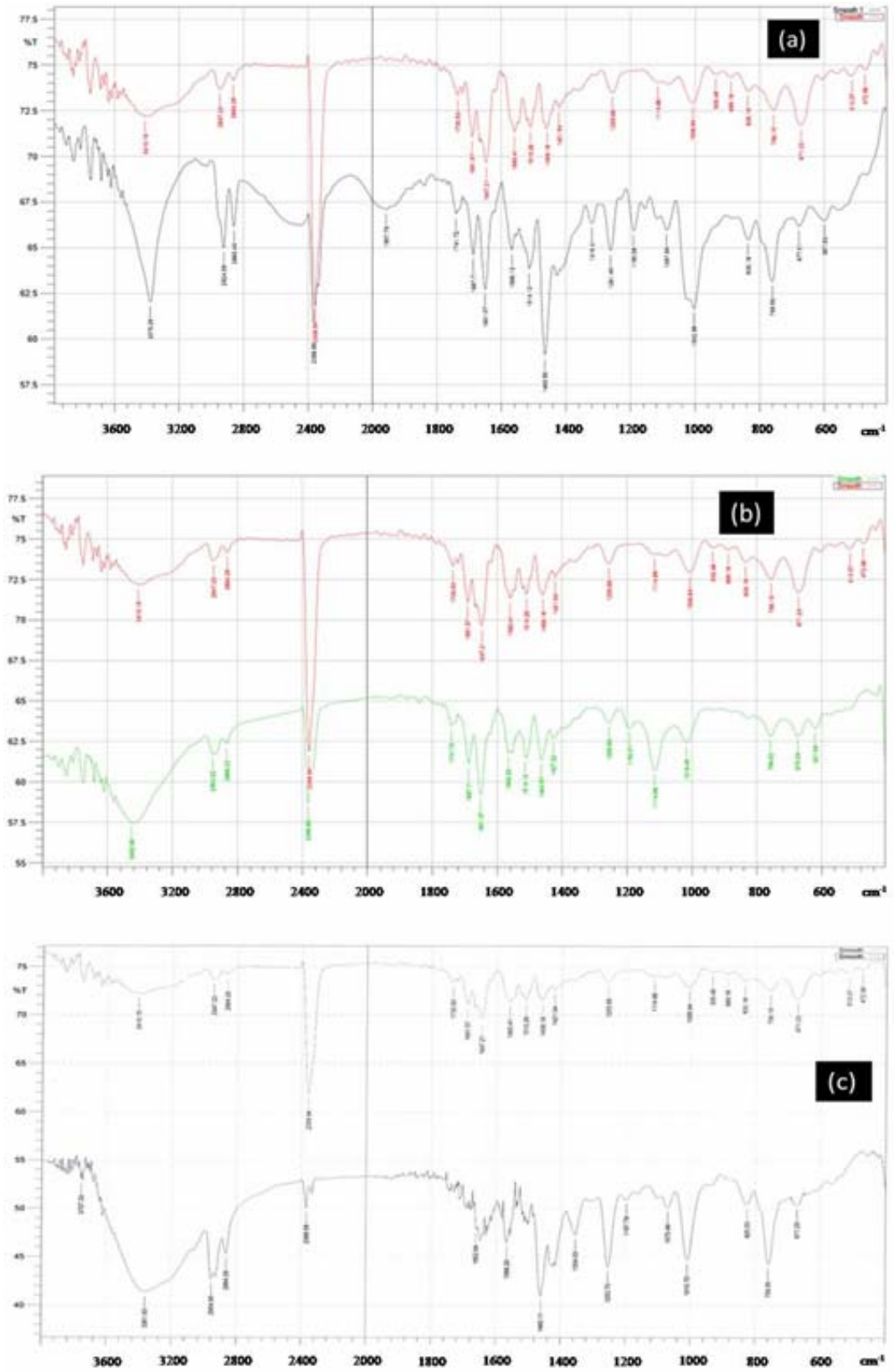

Fig. 1: FTIR spectra of (a) LS-K (top curve) and LS-H (bottom curve), (b) LS-K (top curve) and LS-Cu (II) complex (bottom curve) and, (c) LS-K (top curve) and LS-Ni (II) complex (bottom curve)

bands (fig. 1a). These bands did not appear in the spectrum of complexes of Cu^{+2}, Ni^{+2} (figs. 1b, 1c) and potassium salt of LS as expected and also reported in earlier literature (Etcheverry *et al*., 2007). The infrared absorption bands appeared at 1105 and 1113 cm^{-1} in the spectra of complexes as well as in (LS-K) may be explained by the argument that these bands are shifted from the region at 1087 cm^{-1} as this band appeared in the spectra of (LS-H) at 1087 cm^{-1} (fig. 1a). Both bands at 1105 and 1113 cm^{-1} possess low intensity, likely due to the co-ordination of this fragment of LS molecule to the metal center. Some shifts and changes in the intensities of bands associated to the aromatic ring in the range of 1000-750 cm^{-1} were also observed.

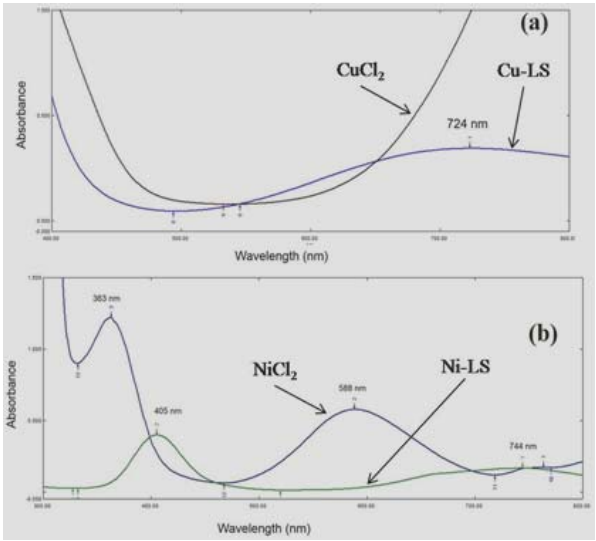

Fig. 2: UV-visible spectra of (a) $CuCl_2$ and Cu-LS complex and (b) $NiCl_2$ and Ni-LS complex.

UV-Visible spectra

Fig. 2a and b show the UV-Visible spectra of LS and its metal complexes recorded in DMSO. LS showed one peak at 230 nm which corresponds to the π to π* transition. In case of $CuCl_2$ (fig. 2a), its d^9 system permitted only one $^2T_{2g}$ to ^2E_g transition which was not observed in the range of 200 to 800 nm explored. This transition, however, was observed at 724 nm in the spectrum of complex (fig. 2a) which indicated the formation of complex. In case of nickel chloride in methanol, two bands appeared at 405 and 744 nm which are corresponded to $^3A_{2g}$ to $^3T_{1g}$ and $^3A_{2g}$ to $^3T_{2g}$ transitions, respectively (fig. 2b). Remarkably, in the spectrum of nickel complex with LS, these bands shifted to lower wavelengths 380 and 600 nm, respectively, (fig. 2b) which supported the successful formation of the complex.

^{1}H-NMR spectra

^{1}H-NMR spectra of LS-K and the synthetic complexes were recorded to obtain a deeper insight into the environment of proton around metal ions in the complex. The resulting spectra are presented in fig. 3. In the spectrum of Cu^{2+} complex, a broad singlet appeared at δ 0.769 was assigned to the proton at C-1, nonetheless, this proton was appeared as a triplet in the spectrum of pure LS. Similarly, sextet, quintet and doublet observed for protons at C-2, C-3 and C-8, respectively, were appeared a broad singlet at δ 1.218, 1.441 and 4.331, respectively. A sharp singlet corresponds to C-9 proton in the spectra of pure LS appeared as a broad singlet at δ 5.198 in the spectrum of complex, while rest of the aromatic protons in copper complex appeared in the range δ 6.635-7.548 as broad singlet. ^{1}H-NMR of nickel complex of LS did not provide sufficient information about the environment of the proton. Nevertheless, all aliphatic protons disappeared and only two protons of the aromatic ring were visible in the range δ 6.589-8.184. The spectra of LS and its copper and nickel complexes are shown in fig. 3a, b, and c with the labeled molecule of LS-K depicted in Scheme 1.

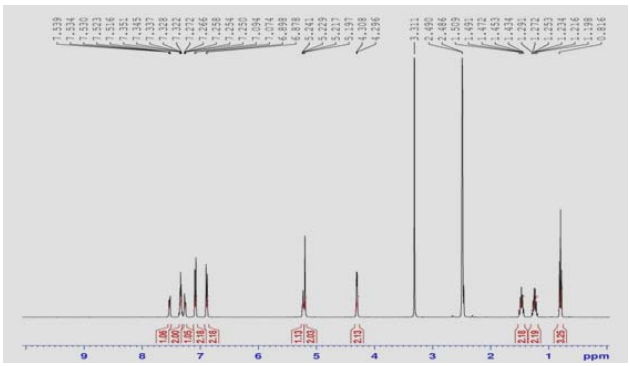

Fig. 3a: ^{1}H-NMR Spectra of LS-K.

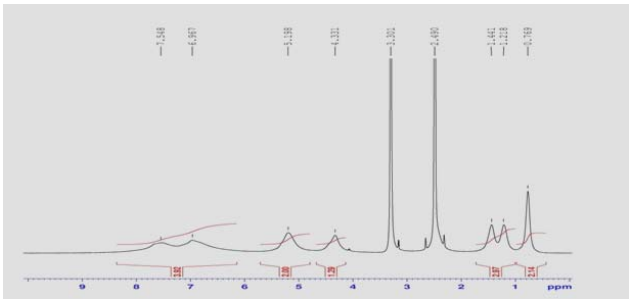

Fig. 3b: ^{1}H NMR Spectra of LS-Cu.

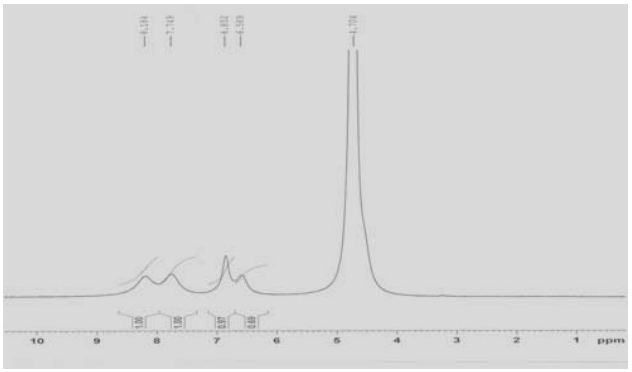

Fig. 3c: ^{1}H NMR Spectra of LS-Ni.

Scanning electron microscope (SEM) images of LS & LS -metal complexes

To explore the possible morphological changes due to complex formation, scanning electron microscopy (SEM) was performed on pure LS and its metal complexes. This technique is considered to be a fundamental and well-suited investigative tool to explore the surface morphologies and particle size distributions of a wide range of micro- and nano-materials such as drug metal complexes. Although SEM does not completely confirm successful complex formation, it can help identifying the existence of a single phase pointing towards a possible complex formation. SEM experiments can also provide key information about the morphology of the crystals at the micro- and nano-meter scale.

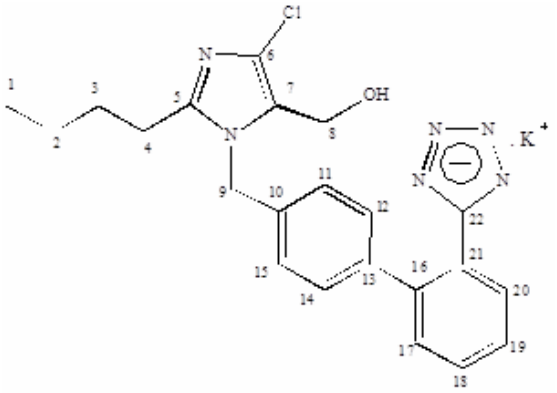

Scheme 1: Labeled losartan potassium.

The micrographs for pure LS are shown in fig. 4a where it appeared as aggregates of large and small rock like large crystalline particles of rather irregular size and a broad size distribution which is in good agreement with micrographs of LS reported in literature (Panneerselvam *et al*., 2010). The micrographs for LS complexes with Ni and Cu are shown in figs. 4b and 4c, respectively. The particles of Ni complex exhibit a non-spherical, platelet-shaped morphology comprising of irregular shaped particles of size ranges in few microns (fig. 4b). Few small particles with the size ranges in nanometers are also visible. The particles exhibit a uniform matrix free from traces of free metal particles which leads us to believe that the material is likely in a homogeneous phase and the complex formation was successful (Malik *et al*., 2015). Contrary to what was observed for pure LS and its Ni complex, the morphology of Cu complex appeared as small particles with size ranges in nanometers and a relatively uniform size distribution (fig. 4c). The particles appeared to have a tendency of aggregation which may likely arise due to artifact of sample preparation before SEM imaging. The surface of the particles, however, is free from any shadow of the metal ions which generally give a sharp contrast in electron microscopy imaging. A complete complex formation and a uniform distribution of drug at the molecular level can be inferred from the homogeneous matrix of the particles (Malik and Wankhede 2015).

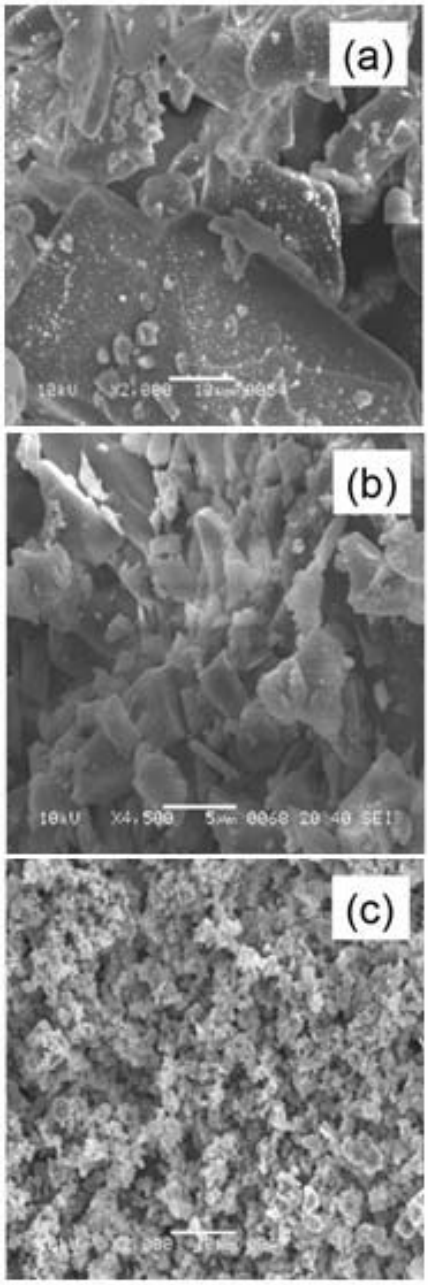

Fig. 4: Scanning Electron Micrographs of (a) pure LS, (b) Ni(II)-LS and (c) Cu(II)-LS.

X-Ray diffraction

X-ray diffraction technique was employed to elucidate the physicochemical state of the losartan potassium (LS) and its metal complexes. The X-ray diffraction patterns of LS and its metal complexes are presented in fig. 5. As shown in fig. 5a, along with several small spikes, XRD pattern of pure LS exhibit some distinct crystalline peaks in the range of 2θ explored (10-60°) indicating it to be likely a mixture of amorphous and polycrystalline forms (Latha *et al*., 2011). The X-ray patterns of LS metal complexes Cu(II)-LS and Ni(II)-LS are shown in fig. 5b and 5c, respectively. These patterns showed no crystalline peaks

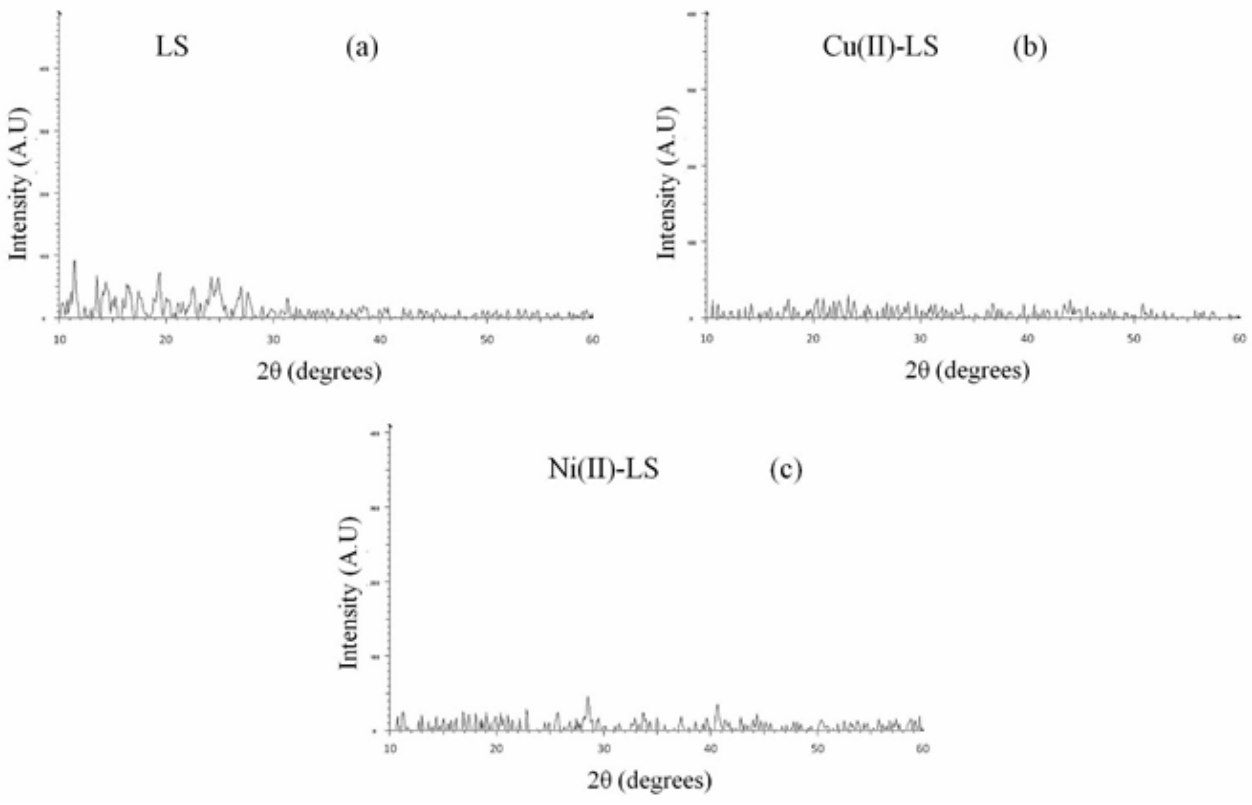

Fig. 5: X-ray diffractograms of (a) pure LS, (b) Cu (II)-LS and (c) Ni (II)-LS.

indicating them to be comprises of amorphous materials. The crystalline peaks of LS were also not observed which indicates that these complexes represent a definite compound of a definite structure and not merely the mixture of the starting materials (Gu *et al.,* 1995).

Cytotoxicity

When the anticancer activity of LS and its Cu(II) and Ni(II) complexes were studied only LS showed slight cytotoxic effects with similar IC_{50} value (mean ± standard deviation) of 88.66±7.33 against cervix carcinoma KB-3-1 cell line. The obtained results are summarised in table 3.

CONCLUSION

In the current study, the synthesis, characterization and cytotoxic activity evaluation of copper and nickel complexes of LS were carried out. The physicochemical characterizations of these complexes were performed including melting point, solubility, BM value, pH, and conductivity measurements. For the structure elucidation, FTIR and ^{1}H-NMR spectroscopic techniques were used. The morphology was studied using the scanning electron microscopy. It was found that these complexes can be formulated as $[Ni(LS)_2Cl_2].H_2O$ and $[Cu(LS)_2Cl_2].6H_2O$. Spectroscopic techniques revealed that both complexes possess an octahedral geometry. Morphological characterizations revealed marked differences in the morphology of pure LS and its metal complexes. Pure LS appeared as aggregates of rock-like large crystalline particles. The Ni complex exhibit a non-spherical, platelet-shaped morphology and Cu complex appeared as small nano-particles. These changes are likely attributed to the complex formation. In the XRD patterns of the complexes, absence of crystalline peaks of LS indicates that these complexes are likely to be new compounds and not merely the mixture of the starting materials.

In conclusion, we have demonstrated the successful formation of LS complexes with Cu and Ni and evaluated their structure and cytotoxic activity. The study gives a detailed knowledge of the new structures for coordination chemistry. This work may be considered as a contribution to understand the formation of metal (II)-LS complexes. We believe that the present contribution will stimulate further research to explore newly prepared complexes in other biological testing to discover potential biological applications as metal-based drugs.

REFERENCES

Alomar K, Landreau A, Allain M, Bouet G and Larcher G (2013). Synthesis, structure and antifungal activity of thiophene-2, 3-dicarboxaldehyde bis (thiosemicarbazone) and nickel (II), copper (II) and cadmium (II) complexes: Unsymmetrical coordination mode of nickel complex. *J. Inorg. Biochem.,* **126**: 76-83.

Andrews RK BR, Zerner B, Sigel H and Sigel A (1988). Metal Ions in Biological Systems, Marcel Dekker Inc., New York, USA.

Belicchi FM, Bisceglie F, Gasparri FG, Pelosi G, Tarasconi P, Albertini R and Pinelli S (2002). Synthesis, characterization and biological activity of two new polymeric copper (II) complexes with alpha-ketoglutaric acid thiosemicarbazone. *J. Inorg. Biochem.,* **89**(1-2): 36-44.

Brazy PC, Stead WW and Fitzwilliam JF (1989). Progression of renal insufficiency: Role of blood pressure. *Kidney Int.,* **35**(2): 670-674.

Campese VM BR (1991). Clinical Factors in Progressive Renal Injury. *Am. J. Kidney Dis.,* **17**: 43.

Carmichael J, DeGraff WG, Gazdar AF, Minna JD and Mitchell JB (1987). Evaluation of a tetrazolium-based semiautomated colorimetric assay: Assessment of chemosensitivity testing. *Cancer Res.,* **47**(4): 936-942.

Chauhan VP, Martin JD, Liu H, Lacorre DA, Jain SR, Kozin SV, Stylianopoulos T, Mousa AS, Han X and Adstamongkonkul P (2013). Angiotensin inhibition enhances drug delivery and potentiates chemotherapy by decompressing tumour blood vessels. *Nat. Commun.,* **4**: 2516.

Dickstein K, Chang P, Willenheimer R, Haunsø S, Remes J, Hall C and Kjekshus J (1995). Comparison of the effects of losartan and enalapril on clinical status and exercise performance in patients with moderate or severe chronic heart failure. *J. Am. Coll Cardiol*., **26**(2): 438-445.

Etcheverry SB, Ferrer EG, Naso L, Barrio DA, Lezama L, Rojo T and Williams PA (2007). Losartan and its interaction with copper (II): Biological effects. *Bioorganic Med. Chem.,* **15**(19): 6418-6424.

Ferrari MB, Bisceglie F, Pelosi G, Tarasconi P, Albertini R, Bonati A, Lunghi P and Pinelli S (2001). Synthesis, characterisation, X-ray structure and biological activity of three new 5-formyluracil thiosemicarbazone complexes. *J. Inorg. Biochem.,* **83**(2): 169-179.

Griendling KK, Murphy T and Alexander RW (1993). Molecular biology of the renin-angiotensin system. *Circulation*., **87**(6): 1816-1828.

Gu X and Jiang W (1995). Characterization of polymorphic forms of fluconazole using fourier transform Raman spectroscopy. *J. Pharm. Sci*., **84**(12): 1438-1441.

Hannedouche T, Chauveau P, Kalou F, Albouze G, Lacour B and Jungers P (1993). Factors affecting progression in advanced chronic renal failure. *Clin. Nephrol.,* **39**(6): 312-320.

Hsu C-W, Kuo C-F, Chuang S-M and Hou M-H (2013). Elucidation of the DNA-interacting properties and anticancer activity of a Ni (II)-coordinated mithramycin dimer complex. *Biometals*., **26**(1): 1-12.

Iakovidis I, Delimaris I and Piperakis SM (2011). Copper and its complexes in medicine: A biochemical approach. *Mol. Biol. Int.,* Epub 2011 Jun 15.

Johnston CI (1995). Angiotensin receptor antagonists: focus on losartan. *Lancet,* **346**(8987): 1403-1407.

Kurtaran R, Yıldırım LT, Azaz AD, Namli H and Atakol O (2005). Synthesis, characterization, crystal structure and biological activity of a novel heterotetranuclear complex:[NiLPb (SCN) 2 (DMF)(H 2 O)] 2, bis-{[μ-N, N′-bis (salicylidene)-1, 3-propanediaminato-aqua-nickel (II)](thiocyanato)(μ-thiocyanato)(μ-N, N′-dimethylformamide) lead (II)}. *J. Inorg. Biochem.*, **99**(10): 1937-1944.

Lacourcière Y, Brunner H, Irwin R, Karlberg BE, Ramsay LE, Snavely DB, Dobbins TW, Faison EP, Nelson EB and Group LCS (1994). Effects of modulators of the renin-angiotensin-aldosterone system on cough. *J Hypertens.,* **12**(12): 1387-1394.

Latha K, Uhumwangho M, Sunil S, Srikanth M and Murthy KR (2011). Development of an optimised losartan potassium press-coated tablets for chronotherapeutic drug delivery. *Trop. J. Pharm Res.,* **10**(5): 551-558.

Malik S and Wankhede S (2015). Synthesis, Characterization and Biological Activity of FE-III and CO-II Complexes Derived from 4-Chloro-2-[(2-Furanylmethyl)-Amino]-5 Sulfamoylbenzoic Acid. *Int J. Appl. Biol. Pharm.,* **6**(2): 205-210

Mehta PK and Griendling KK (2007). Angiotensin II cell signaling: Physiological and pathological effects in the cardiovascular system. *Am. J. Physiol. Cell Physiol.,* **292**(1): 82-97.

Meyer F KH, McCleverty JA and Meyer TJ (2003). Comprehensive Coordination Chemistry II, Elsevie.

Osredkar J and Sustar N (2011). Copper and zinc, biological role and significance of copper/zinc imbalance. *J. Clinic. Toxicol.*, **3**: 001.

Panneerselvam M, Natrajan R, Selvaraj S and Rajendran N (2010). A Novel Drug-Drug Solid Dispersion of Hydrochlorothiazide losartan Potassium. *Int. J. Pharma. Bio. Sci.,* **1**(4): 68-80.

Qin Z (2008). Newly developed angiotensin II-infused experimental models in vascular biology. *Regul Pept*., **150**(1): 1-6.

Rhodes DR, Ateeq B, Cao Q, Tomlins SA, Mehra R, Laxman B, Kalyana-Sundaram S, Lonigro RJ, Helgeson BE and Bhojani MS (2009). AGTR1 overexpression defines a subset of breast cancer and confers sensitivity to losartan, an AGTR1 antagonist. *Proc. Natl. Acad. Sci.,* **106**(25): 10284-10289.

Rodrıguez-Argüelles MC, Ferrari MB, Bisceglie F, Pelizzi C, Pelosi G, Pinelli S and Sassi M (2004). Synthesis, characterization and biological activity of Ni, Cu and Zn complexes of isatin hydrazones. *J. Inorg. Biochem.,* **98**(2): 313-321.

Sathyadevi P, Krishnamoorthy P, Jayanthi E, Butorac RR, Cowley AH and Dharmaraj N (2012). Studies on the effect of metal ions of hydrazone complexes on interaction with nucleic acids, bovine serum albumin

and antioxidant properties. *Inorganica Chimica Acta* **384**: 83-96.

Shawish HB, Wong WY, Wong YL, Loh SW, Looi CY, Hassandarvish P, Phan AYL, Wong WF, Wang H and Paterson IC (2014). Nickel (II) complex of polyhydroxybenzaldehyde N4-thiosemicarbazone exhibits anti-inflammatory activity by inhibiting NF-κB transactivation. *PloS one*., **9**(6): e100933.

Ska DA, Lo M-W, Shaw WC, Keane WF, Gehr TW, Halstenson CE, Lipschutz K, Furtek CI, Ritter MA and Shahinfar S (1995). The pharmacokinetics of losartan in renal insufficiency. *J. Hypertens.,* **13**: 49-52.

Skyrianou KC, Efthimiadou EK, Psycharis V, Terzis A, Kessissoglou DP and Psomas G (2009). Nickel-quinolones interaction. Part 1-Nickel (II) complexes with the antibacterial drug sparfloxacin: Structure and biological properties. *J. Inorg. Biochem.,* **103**(12): 1617-1625.

Skyrianou KC, Perdih F, Papadopoulos AN, Turel I, Kessissoglou DP and Psomas G (2011). Nickel-quinolones interaction: Part 5-Biological evaluation of nickel (II) complexes with first-, second-and third-generation quinolones. *J. Inorg. Biochem.,* **105**(10): 1273-1285.

Tedesco M, Ratti G, Aquino D, Limongelli G, Salvo GD, Mennella S, Galzerano D, Iarussi D and Iacono A (1998). Effects of losartan on hypertension and left ventricular mass: A long-term study. *J. Hum. Hypertens.,* **12**(8): 505-510.

Timmermans PB CD and Chiu AT (2009). Nonpeptide Angiotensin II Receptor Antagonists. *Am. J. Hypertens.,* **3**: 599.

Walker WG (1993). Hypertension-related renal injury: A major contributor to end-stage renal disease. *Am. J. Kidney Dis*., **22**(1): 164-173.

Wong PC, Hart SD, Chiu AT, Herblin WF, Carini DJ, Smith RD, Wexler R and Timmermans PB (1991). Pharmacology of DuP 532, a selective and noncompetitive AT1 receptor antagonist. *J. Pharmacol. Exp. Ther.,* **259**(2): 861-870.

Wong PC, Price W, Chiu AT, Duncia JV, Carini DJ, Wexler RR, Johnson AL and Timmermans PB (1990). Nonpeptide angiotensin II receptor antagonists. XI. Pharmacology of EXP3174: An active metabolite of DuP 753, an orally active antihypertensive agent. *J. Pharmacol. Exp. Ther.,* **255**(1): 211-217.

Yesilel OZ, Soylu MS, Ölmez H and Buyukgungor O (2006). Synthesis and spectrothermal studies of vitamin B13 complexes of cobalt (II) and nickel (II) with 4-methylimidazole: Crystal structure of $[Ni(HOr)(H_2O)(4\text{-}Meim)_3]_2 \cdot 5H_2O$. *Polyhedron,* **25**(15): 2985-2992.